fuels

MDPI

Article

Biogas Dry Reforming for Hydrogen through Membrane Reactor Utilizing Negative Pressure

Akira Nishimura [1,*], Tomohiro Takada [1], Satoshi Ohata [1] and Mohan Lal Kolhe [2]

[1] Division of Mechanical Engineering, Graduate Shool of Engineering, Mie University, Tsu, Mie 514-8507, Japan; nisiaki531@ybb.ne.jp (T.T.); 420m111@m.mie-u.ac.jp (S.O.)
[2] Faculty of Engineering & Science, University of Agder, 4879 Grimstad, Norway; mohan.l.kolhe@uia.no
* Correspondence: nisimura@mach.mie-u.ac.jp; Tel.: +81-59-231-9747

Abstract: Biogas, consisting of CH_4 and CO_2, is a promising energy source and can be converted into H_2 by a dry reforming reaction. In this study, a membrane reactor is adopted to promote the performance of biogas dry reforming. The aim of this study is to investigate the effect of pressure of sweep gas on a biogas dry reforming to get H_2. The effect of molar ratio of supplied CH_4:CO_2 and reaction temperature is also investigated. It is observed that the impact of p_{sweep} on concentrations of CH_4 and CO_2 is small irrespective of reaction temperature. The concentrations of H_2 and CO increase with an increase in reaction temperature $_t$. The concentration of H_2, at the outlet of the reaction chamber, reduces with a decrease in p_{sweep}. It is due to an increase in H_2 extraction from the reaction chamber to the sweep chamber. The highest concentration of H_2 is obtained in the case of the molar ratio of CH_4:CO_2 = 1:1. The concentration of CO is the highest in the case of the molar ratio of CH_4:CO_2 = 1.5:1. The highest sweep effect is obtained at reaction temperature of 500 °C and p_{sweep} of 0.045 MPa.

Keywords: biogas dry reforming; membrane reactor; Ni catalyst; pressure difference provided by vacuum pump; initial temperature for dry reforming; molar ratio of CH_4:CO_2

Citation: Nishimura, A.; Takada, T.; Ohata, S.; Kolhe, M.L. Biogas Dry Reforming for Hydrogen through Membrane Reactor Utilizing Negative Pressure. *Fuels* **2021**, *2*, 194–209. https://doi.org/10.3390/fuels2020012

Academic Editor: Timothy Lipman

Received: 1 April 2021
Accepted: 17 May 2021
Published: 19 May 2021

1. Introduction

Global warming problem is a serious issue in the world. Each country has set the goal to reduce CO_2 emission, by 2030 or 2050. For instance, the Japan had declared to reduce the amount of CO_2 emission up to zero practically by 2050. Though there are many ways to reduce the amount of CO_2 emission, such as a digested sewage sludge for CO_2 removal from biogas [1] and a production of high-quality hydrocarbon fuel from palm waste [2], a renewable H_2 is a promising candidate. Renewable H_2, which is called a green H_2, can assist to solve the global warming and construct an energy supply chain to meet the increasing energy demand. There are some innovative approaches for green H_2 production. H_2 production by the water splitting over Fe_3O_4 pellet at low temperature of 250 °C, 290 °C and 310 °C [3] and photothermal-photocatalytic materials under light illumination without additional energy [4] were reported. In addition, the anion exchange membrane (AEM) electrolysis for large-scale H_2 production was investigated to clarify the resistances involved in AEM electrolysis [5].

This study focuses on H_2 produced from a biogas dry reforming. Biogas is a gaseous fuel consisting of CH_4 (55–75 vol%) and CO_2 (25–45 vol%) [6], mainly produced from fermentation by the action of anaerobic microorganisms on raw materials such as, garbage, livestock excretion, and sewage sludge. Additionally, the conversion of biogas to H_2 can be said as a carbon neutral since the CO_2, which is a by-product in the biogas production process, can be absorbed by plants. It is known from the International Energy Agency (IEA) [7] that the biogas has been produced 59.3 billion m^3 globally with an equivalent energy of 1.36 EJ in 2018, which is approximately five times as large as that in 2000. Therefore, a biogas is thought to be a promising energy source.

It is generally known that a biogas is used as a fuel for gas engine or micro gas turbine [8]. Biogas contains CO_2 of approximately 40 vol% which reduces the heating value compared to a natural gas, resulting in the efficiency of power generation decreasing. Considering it, this study focuses on a biogas dry reforming to produce H_2, which can be used as a fuel in the fuel cell system, such as solid oxide fuel cell (SOFC). Biogas dry reforming has been studied previously by several researchers [9–27]. The catalyst development, which is one of important issues, is investigated to improve the performance of biogas dry reforming. Several catalysts such as Co-Ni/Al_2O_3, Ce-Co-Ni/Al_2O_3 [9], Pt-Ni/YSZ [10], Ni/Ce/$MgAl_2O_4$ [11], Pt-Ni/Al_2O_3 [12], La-La_2O_3/-Ni [13], Pd-Ni-Mg/Ceria-Zirconia [14], Ni/γ-Al_2O_3 [15], Ni/SBA-15 [16], Ni/ZnO-Al_2O_3 [17], Ni/CeO_2-SiO_2 [18], Ni/ZrO_2 [19], Ni/CaZrNiOx [20], Ni/$CaFe_2O_4$ [21], Ni/Ce/TiO_2-Al_2O_3 [22], Ni nanoparticle [23], Ni/ZnO-CeO_2 [24], Rh/Ni [25], Ni-based bimodal porous catalyst [26] and Cu/Ni bimetallic catalyst [27] have been investigated, resulting that Ni-based catalyst is the most common catalyst for the biogas dry reforming process. Therefore, Ni catalyst is adopted in this study. In addition, a membrane reactor is also adopted to improve the efficiency of biogas dry reforming in this study. It is well-known that a membrane reactor is used to improve the CH_4 steam reforming by separating H_2 from the reaction space [28–30] as soon as it is produced. The synergetic effect of the membrane reactor on performing the reaction and the separation in the same unit should be analyzed. It requires advanced levels of automation and control to re-design process [31]. Pd based membrane is used to separate H_2 due to its high efficiency [31–33]. According to the literature survey, Pd membrane has been used to improve the performance of CH_4 dry reforming [34–44]. The coupled effect of membrane and catalyst on CH_4 conversion has been discussed earlier [31]. Alloy membrane such as Pd/Ag [34–36], Pd/Au [37,38] and Pd/Cu [39,40] have been used generally due to the stability at high temperature [32]. Hollow fiber membrane reactor can perform CH_4 conversion, which has higher by 72 % output than traditional fixed bed reactor [41]. The Pd/Au alloy membrane has been used in the two-zone fluidized bed reactor [33,42] and showed CH_4 conversion and H_2 selectivity to be higher compared to the conventional fluidized bed reactor. Reaction combination consisting of dry reforming and steam reforming has been carried out in a Pd/Ag membrane reactor, resulting that CH_4 conversion above 90% has achieved at 650 °C [36]. The effect of flow rate of sweep gas on CH_4 conversion has been investigated by two membrane reactors, equipped with the expensive dense H_2 selective membrane and the inexpensive porous Vycor glass membrane [43]. There has been a significant loss of the reactant with an increase in sweep gas flow rate, which in turn can decrease the CH_4 conversion. The other study [35], which has investigated the effect of flow rate of sweep gas and reported that CH_4 conversion and H_2 recovery have increased with an increase in the flow rate of sweep gas. In addition, it is also reported that the increase in reaction pressure has showed the negative effect on CH_4 conversion at the reaction temperature of 550 °C [35]. However, the other study [44] has reported a contrary conclusion that in CH_4 conversion, H_2 recovery and H_2/CO ratio have increased with an increase in reaction pressure at the reaction temperature of 800 °C. It [44] has also reported that H_2/CO ratio has decreased with the increase in CO_2/CH_4 ratio. Since the H_2 flux through membrane has increased with transmembrane pressure difference [34], it is expected that the performance of biogas dry reforming has been improved due to the shift of the reaction toward further conversion [31]. Though the impact of negative pressure of sweep gas on H_2 diffusion flux has been reported [45], and at this moment, there is no study investigating the effect of negative pressure of sweep gas on the performance of biogas dry reforming.

Therefore, the aim of this study is to understand the effect of pressure of sweep gas (p_{sweep}) on the performance of the biogas dry reforming process. In this study, the pressure difference was provided by vacuum pomp as the negative pressure. The effect of changing reaction temperature, which means the initial temperature for dry reforming in this study, from 400 °C to 600 °C, and the molar ratio of CH_4:CO_2 by 1.5:1, 1:1 and 1:1.5 is also investigated. The molar ratio of CH_4:CO_2 = 1.5:1 simulates a biogas. Since a pure

Pd membrane has relatively high solubility for carbon, it causes membrane degradation leading to the loss of permeability [46]. Therefore, the Pd/Cu alloy membrane is used in this study. The reaction scheme of CH_4 dry reforming is as follows:

$$CH_4 + CO_2 \leftrightarrow 2CO + 2H_2 \quad (1)$$

The other reaction schemes which can be thought to be occurred in this study are as follows [32]:

$$CO_2 + H_2 \leftrightarrow CO + H_2O \quad (2)$$

$$CH_4 + H_2O \leftrightarrow CO + 3H_2 \quad (3)$$

$$CO_2 + 4H_2 \leftrightarrow CH_4 + 2H_2O \quad (4)$$

where Equation (2) is the reverse water gas shift reaction (RWGS), Equation (3) is steam reforming of CH_4 and Equation (4) is the methanation reaction.

2. Experimentation

2.1. Experimental Set-Up

Figure 1 illustrates the schematic drawing of experimental set-up used in this study. The experimental apparatus is composed of a gas cylinder, mass flow controllers (S48–32; produced by HORIBA METRON INC., Shanghai, China), pressure sensors (KM31; produced by NAGANO KEIKI, Tokyo, Japan), valves, a vacuum pump, a Pirani gauge (SW-1; produced by ULVAC, Saito-City, Miyazaki, Japan) for measuring negative pressure, a reactor consisting of reaction chamber and sweep chamber, and gas sampling taps. The reactor is in the furnace. The temperature in the furnace is controlled by far-infrared heaters (MCHNNS1; produced by MISUMI, Tokyo, Japan). CH_4 gas whose purity is over 99.4 vol% and CO_2 gas whose purity is over 99.9 vol% are controlled by the mass flow controllers and mixed before the reactors. The pressure of the mixed gas is measured by pressure sensors. Ar gas whose purity is over 99.99 vol% is controlled by the mass flow controller, and the pressure of Ar gas is measured by the pressure sensor, which is supplied as a sweep gas. The exhausted gas at the outlet of the reactor is suctioned by a gas syringe via the gas sampling tap. The concentration of sampled gas is measured by FID gas chromatography and a methanizer whose minimum resolution of both FID gas chromatograph and methanizer is 1 ppmV. The gas pressure at the outlet of the reactor is measured by the pressure sensor. The gas concentration and pressure are measured at the outlet of the reaction chamber and sweep chamber, respectively. A valve is installed next to the pressure gauge at the outlet of the reaction chamber to investigate the effect of p_{sweep} on the performance of CH_4 dry reforming. When the valve is closed, the gas in the reaction chamber flows to the sweep chamber preferentially.

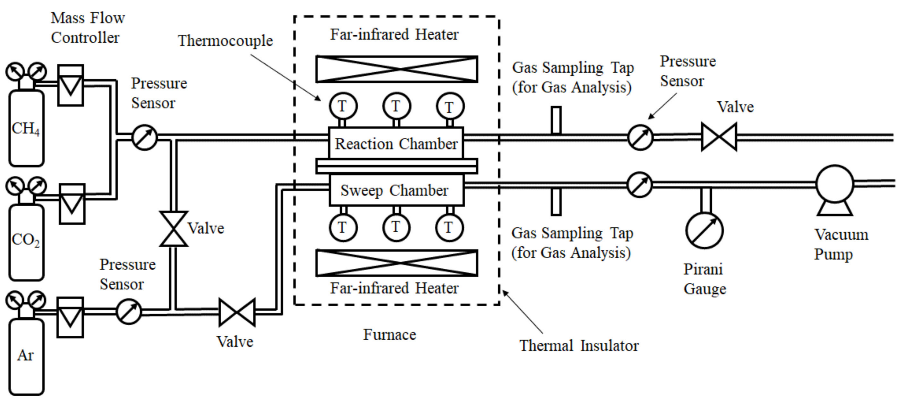

Figure 1. Schematic of experimental set-up.

Figure 2 shows the detail and photo of the reactor. The reactor is composed of a reaction chamber, a sweep chamber, and anH_2 separation membrane. The reaction chamber and the sweep chamber are made of stainless steel, which has a size of 40 mm × 100 mm × 40 mm. The reaction space has a volume of 16×10^{-5} m^3. Porous pure Ni catalyst is placed in the reaction chamber. The average pore diameter of the catalyst is 1.9 mm. The weight of the catalyst is 63.1 g. The Pd/Cu alloy membrane (Cu of 40 wt%; produced by Tanaka Kikinzoku Kogyo, Tokyo, Japan) installed between reaction and separation chambers can provide H_2 separation. The thickness of the Pd/Cu alloy membrane is 60 μm. The temperatures at the inlet, middle, and outlet of the reaction and sweep chambers are measured using K-type thermocouples. The measured temperature and pressure are collected by the data logger (GL240; produced by Graphtec Corporation, Kanagawa, Japan).

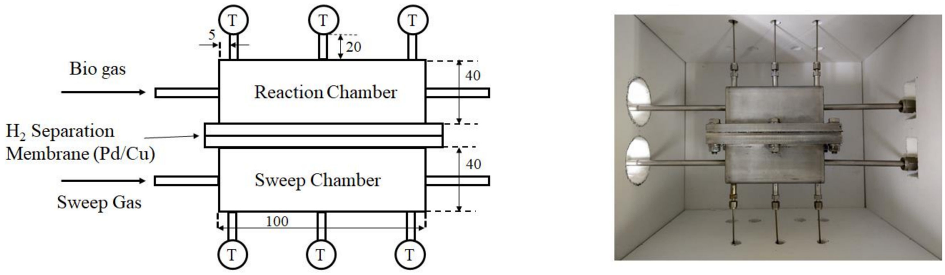

Figure 2. Schematic detail and photo of reactor.

Table 1 lists the experimental parameters in this study. The molar ratio of the supplied CH_4:CO_2 is changed at 1.5:1, 1:1 or 1:1.5, where CH_4:CO_2 = 1.5:1 simulates a biogas. The feed ratio of sweep gas, defined as the flow rate of sweep gas divided by the flow rate of supply gas composed of CH_4 and CO_2 is set at 1.0 since the best performance of CH_4 dry reforming was obtained at the feed ratio of sweep gas at 1 according to the authors' previous study [47]. The pressure in the sweep chamber is changed by 0.10 MPa, 0.09 MPa and 0.045 MPa by means of vacuum pump and Pirani gauge. The effect of molar ratio on the performance of CH_4 dry reforming has been investigated changing the reaction temperature of 400 °C, 500 °C and 600 °C. The gas concentrations in reaction and sweep chambers have been evaluated by FID gas chromatograph (produced by GL Science, Nishi Shinjuku, Japan) and methanizer (produced by GL Science). This study shows the average data of five trials for each experimental condition in the following figures. The distribution of each gas concentration has been below 10 %. H_2 selectivity and CO selectivity have also been evaluated.

Table 1. Experimental parameters.

Reaction temperature (°C)	400, 500, 600
Pressure of supply gas (MPa)	0.10
Pressure of sweep gas, p_{sweep} (MPa)	0.10, 0.09, 0.045
Temperature of supply gas (°C)	25
Molar ratio of supplied CH_4:CO_2	1.5:1, 1:1, 1:1.5
(Flow rate of CH_4 and CO_2 (NL/min))	(1.088:0.725, 0.725:0.725, 0.725:1.088)
Feed ratio of sweep gas	1.0

2.2. Performance Evaluation of Proposed Reactor

The performance of the proposed reactor is evaluated by gas concentration at the outlet of reaction and sweep chambers, H_2 selectivity and CO selectivity. H_2 selectivity (S_{H2}) and CO selectivity (S_{co}) are defined as following:

$$S_{H2} = C_{H2,\,out}/(C_{H2,\,out} + C_{CO,\,out}) \times 100 \quad (5)$$

$$S_{CO} = C_{CO,\,out}/(C_{H2,\,out} + C_{CO,\,out}) \times 100 \quad (6)$$

where S_{H2} is H_2 selectivity (%), $C_{H2,\,out}$ is the concentration of H_2 at the outlet of reaction and sweep chambers (ppmV), $C_{CO,\,out}$ is the concentration of CO at the outlet of reaction chamber (ppmV), and S_{CO} is the CO selectivity (%).

In addition, this study also evaluates the performance of the proposed reactor by CH_4 conversion (X_{CH4}), CO_2 conversion (X_{CO2}) and H_2 yield (Y_{H2}). This study defines X_{CH4} and X_{CO2} following Equation (1). X_{CH4}, X_{CO2} and Y_{H2} are defined as follows:

$$X_{CH4} = (2C_{H2,,out})/(C_{CH4,\,in}) \times 100 \tag{7}$$

$$X_{CO2} = (2C_{CO,\,out})/(C_{CO2,\,in}) \times 100 \tag{8}$$

$$Y_{H2} = (1/2C_{H2,\,out})/(C_{CH4,\,in}) \times 100 \tag{9}$$

3. Results and Discussion

3.1. Effect of Pressure of Sweep Gas on the Performance of Dry Reforming under Different Reaction Temperatures

Figures 3–5 compare relationship between the concentrations of CH_4, CO_2, H_2 and CO at the outlet of the reaction chamber changing reaction temperature, respectively. Reaction temperature is varied to 400 °C, 500 °C, or 600 °C. In these figures, the molar ratio of the supplied CH_4:CO_2 is 1.5:1. In addition, the error bars are also shown in these figures.

It is seen from Figure 3 that the impact of p_{sweep} on concentrations of CH_4 and CO_2 is a little, while the concentration of CH_4 at the reaction temperature of 600 °C decreases with a decrease in p_{sweep}. It is believed that H_2 separation is promoted with a decrease in p_{sweep}, resulting that CH_4 is consumed more. However, it is found from Figure 3 that the change in concentration of CO_2 with increase in reaction temperature is a small. Since the kinetic rates expressed by Arrehenius type of Equations (1), (2) and (4), which consume CO_2 in the reaction, are much smaller than that of Equation (3) [11], it is believed that the impact of the reaction temperature on the concentration of CO_2 is a small. Though this study focuses on CH_4 dry reforming, H_2O, which is the by-product in the reaction as shown in Equation (3), might be produced, resulting that the consumption of CH_4 is larger than that of CO_2 at the reaction temperature of 600 °C due to the higher reaction rate of Equation (3) [11].

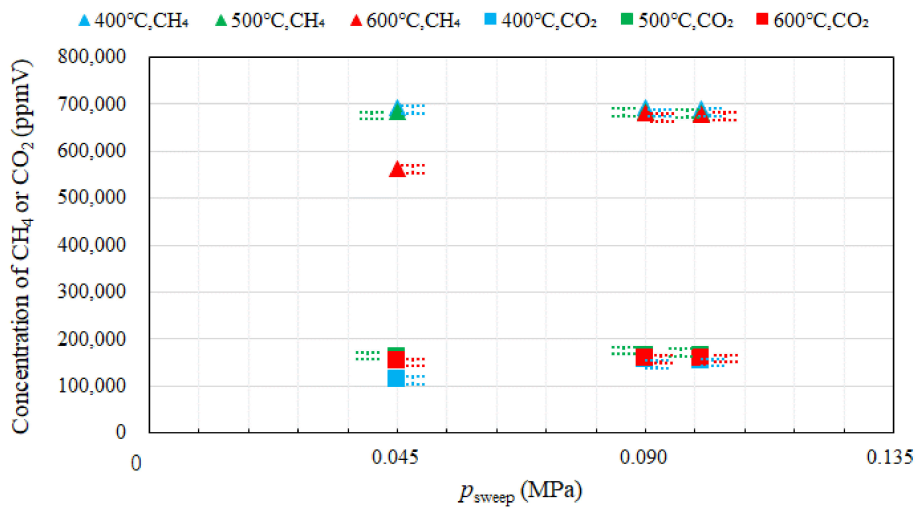

Figure 3. Impact of concentrations of CH_4 and CO_2 at the outlet of reaction chamber and p_{sweep} with change in reaction temperature. (CH_4:CO_2 = 1.5:1).

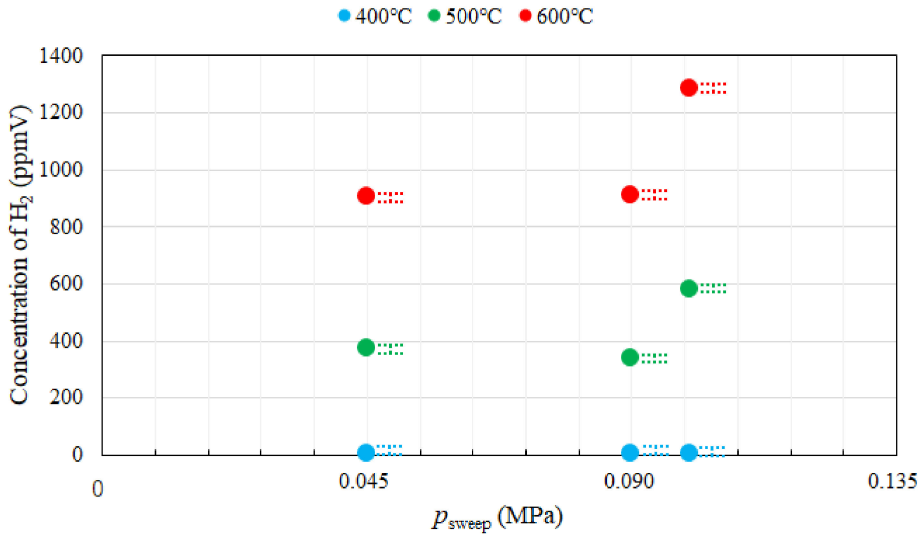

Figure 4. Impact of concentration of H_2 at the outlet of the reaction chamber and p_{sweep} with change in reaction temperature. (CH_4:CO_2 = 1.5:1).

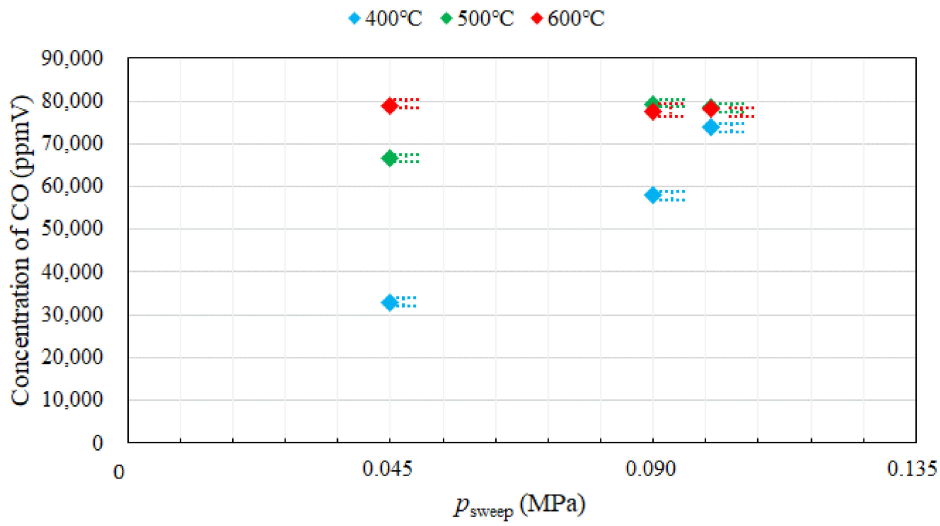

Figure 5. Impact of concentration of CO at the outlet of reaction chamber and p_{sweep} with change in.reaction temperature. (CH_4:CO_2 = 1.5:1).

According to Figures 4 and 5, it is seen that the concentrations of H_2 and CO increase with incases in reaction temperature. According to the theoretical kinetic studies [12,48], the reaction rates of H_2 and CO increase with an increase in reaction temperature, resulting that the concentrations of H_2 and CO increase. This is the same tendency observed in the experimental study using Pd/Ag/Cu membrane changing the reaction temperature from 350 °C to 700 °C [32]. Since reaction temperature is too low, it is believed that H_2 is not produced at the reaction temperature of 400 °C. In addition, it is observed from Figures 4 and 5 that the concentrations of H_2 and CO under negative pressure conditions are lower than those under the atmosphere pressure condition, i.e., p_{sweep} of 0.10 MPa. Since H_2 flux thorough Pd/Cu membrane is improved by increase in the pressure difference between reaction chamber and sweep chamber [45], it is thought that H_2 is moved from the reaction chamber to the sweep chamber. Therefore, the concentration of H_2 under negative pressure conditions is smaller than that under the atmosphere pressure condition. As to

CO, it is believed that the following reaction with H_2O, which is by-product in the reaction shown in Equation (3), might have been occurred [49]:

$$CO + H_2O \leftrightarrow CO_2 + H_2 \tag{10}$$

In addition, the following reactions on carbon deposition are thought to be occurred [32,50,51]:

$$2CO \rightarrow CO_2 + C \tag{11}$$

$$CO + H_2 \rightarrow H_2O + C \tag{12}$$

In this study, it is assumed that the concentration of CO decreases according to the combination of these reactions.

Table 2 lists the relationship between H_2, CO selectivity and p_{sweep}, respectively. Reaction temperature is varied to 400 °C, 500 °C, or 600 °C.

Table 2. Relationship between H_2, CO selectivity and p_{sweep} with change in reaction temperature.

p_{sweep} (MPa)	H_2 Selectivity (%)			CO Selectivity (%)		
	400 °C	500 °C			500 °C	600 °C
0.045	0	0.5	1.1	100	99.5	98.9
0.090	0	0.4	1.2	100	99.6	98.8
0.101	0	0.7	1.6	100	99.3	98.4

According to Table 2, it is revealed that CO is produced mainly irrespective of p_{sweep} changing reaction temperature. Since reaction temperature is relatively low even the reaction temperature of 600 °C and H_2 selectivity increases with an increase in reaction temperature, especially over 600 °C [32], high CO selectivity is noticed in this study.

Tables 3–5 list the relationship between CH_4 conversion, CO_2 conversion, H_2 yield and p_{sweep}, respectively. The reaction temperature is varied to 400 °C, 500 °C, or 600 °C.

Table 3. Relationship between CH_4 conversion and p_{sweep} with change in reaction temperature.

p_{sweep} (MPa)	400 °C (%)	500 °C (%)	600 °C (%)
0.045	0.002	0.129	0.303
0.090	0.002	0.112	0.304
0.101	0.003	0.193	0.429

Table 4. Relationship between CO_2 conversion and p_{sweep} with change in reaction temperature.

p_{sweep} (MPa)	400 °C (%)	500 °C (%)	600 °C (%)
0.045	16.5	35.2	39.4
0.090	29.3	40.1	38.9
0.101	37.0	39.4	39.2

Table 5. Relationship between H_2 yield and p_{sweep} with change in reaction temperature.

p_{sweep} (MPa)	400 °C (%)	500 °C (%)	600 °C (%)
0.045	0.0006	0.0322	0.0758
0.090	0.0005	0.0281	0.0761
0.101	0.0007	0.0483	0.1072

According to Tables 3 and 5, it is seen that CH_4 conversion and H_2 yield are small. It is thought due to low concentration of H_2 as shown in Figure 4. It is also seen from Tables 3 and 4 that CO_2 conversion is larger compared to CH_4 conversion irrespective of p_{sweep} and reaction temperature, resulting from that the reaction shown by Equations (2) and (4) might be progressed well.

3.2. *Effect of Pressure of Sweep Gas on the Performance of Dry Reforming under Different Molar Ratios*

Figures 6–8 compare the impact of concentrations of CH_4, CO_2, H_2 and CO at the outlet of the reaction chamber with changing the molar ratio of CH_4:CO_2. The molar ratio of CH_4:CO_2 is varied to 1.5:1, 1:1, 1:1.5. In these figures, the reaction temperature is 500 °C. In addition, the error bars are also shown in these figures.

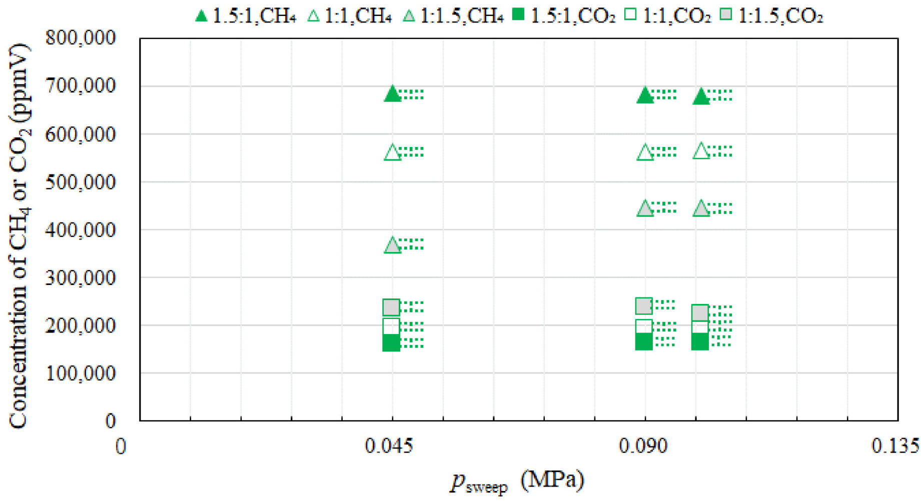

Figure 6. Impact of concentrations of CH_4 and CO_2 at the outlet of reaction chamber on p_{sweep} with changing molar ratios of CH_4:CO_2.

According to Figure 6, it is found that the concentrations of CH_4 and CO_2 are changed with the molar ratio of CH_4:CO_2. In addition, it is seen from Figure 6 that the impact of p_{sweep} on the concentrations of CH_4 and CO is relatively small.

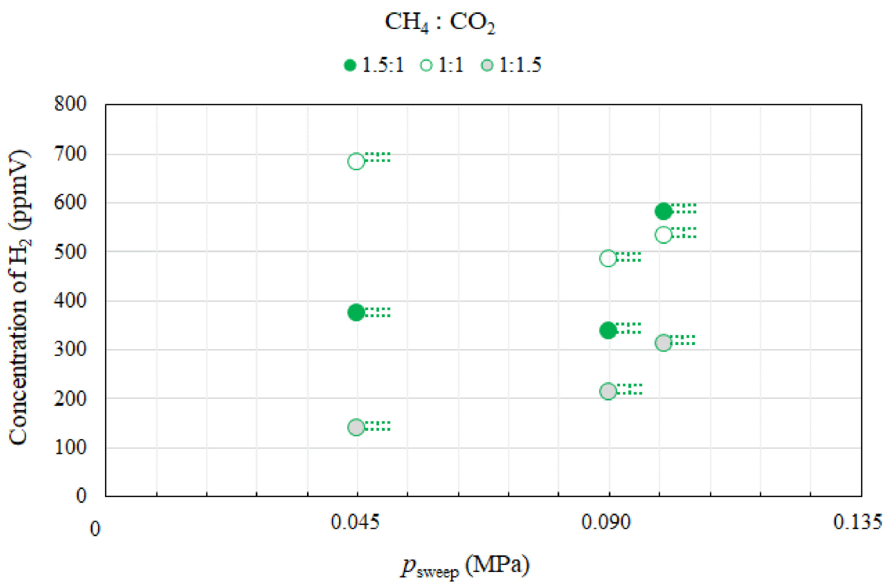

Figure 7. Impact of concentration of H_2 at the outlet of reaction chamber and p_{sweep} with changing molar ratios of CH_4:CO_2.

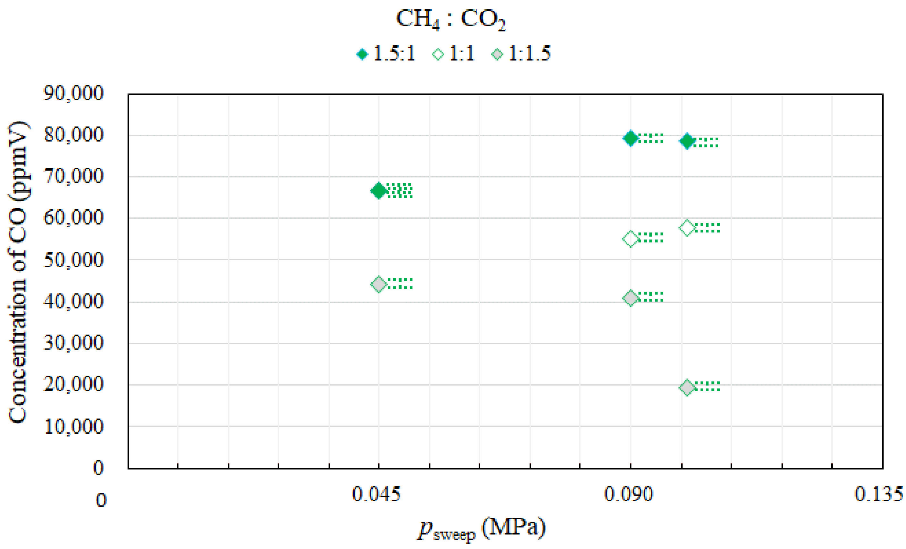

Figure 8. Relationship between concentration of CO at the outlet of reaction chamber and p_{sweep} of with changing molar ratios of CH_4:CO_2.

It is seen from Figure 7 that the concentration of H_2, in the case of the molar ratio of CH_4:CO_2 = 1:1 is the highest among different molar ratio conditions. Since the molar ratio of CH_4:CO_2 = 1:1 is the theoretical stoichiometric ratio according to Equation (1), it is believed that the reaction is progressed. Compared to the concentration of H_2 in the case of the molar ratio of CH_4:CO_2 = 1.5:1 with that in the case of the molar ratio of CH_4:CO_2 = 1:1.5, the former is higher than the latter. When the molar ratio of CH_4 is larger, it is believed that Equation (3) is progressed well after H_2O production by the reactions shown by Equations (2) and (4). In addition, it is observed from Figure 7 that the concentrations of H_2 under negative pressure conditions are lower than those under the atmosphere pressure condition, except for the case of the molar ratio of CH_4:CO_2 = 1:1. Since H_2 flux thorough Pd/Cu membrane is improved by increase in the pressure difference between reaction chamber and sweep chamber [45], it is thought that H_2 is moved from the reaction chamber to the sweep chamber. Therefore, the concentration of H_2 under negative pressure conditions is smaller than that under the atmosphere pressure condition. The amount of produced H_2 might be large in the case of the molar ratio of CH_4:CO_2 = 1:1, and the thickness of Pd/Cu membrane might not be sufficient, resulting that H_2 flux is not sufficient to extract H_2 by Pd/Cu membrane even p_{sweep} at 0.045 MPa.

It is seen from Figure 8 that the concentration of CO in the case of the molar ratio of CH_4:CO_2 = 1.5:1 is the highest among different molar ratio conditions. At the molar ratio of CH_4:CO_2 = 1.5:1, it is believed that Equation (3) is progressed well after H_2O production by the reactions shown by Equations (2) and (4). As a result, the concentration of CO increases in the case of the molar ratio of CH_4:CO_2 = 1.5:1. Additionally, it is observed from Figure 8 that the concentration of CO in the case of the molar ratio of CH_4:CO_2 = 1:1.5 is low at p_{sweep} of 0.10 MPa. Since the performance of dry reforming of CH_4 is worse, and it can not obtain the side-effect of CO production by H_2 separation due to no pressure difference between reaction chamber and sweep chamber, it is believed that the concentration of CO is low under this condition.

Table 6 lists the relationship between H_2, CO selectivity and p_{sweep}. The molar ratio of CH_4:CO_2 is varied to 1.5:1, 1:1, 1:1.5. In this table, the reaction temperature is 500 °C.

Table 6. Relationship between H_2, CO selectivity and p_{sweep} changing molar ratios of CH_4:CO_2.

p_{sweep} (MPa)	H_2 Selectivity (%)			CO Selectivity (%)		
	CH_4:CO_2 = 1.5:1	CH_4:CO_2 = 1:1	CH_4:CO_2 = 1:1.5	CH_4:CO_2 = 1.5:1	CH_4:CO_2 = 1:1	CH_4:CO_2 = 1:1.5
0.045	0.5	1.0	0.3	99.5	99.0	99.7
0.090	0.4	0.9	0.5	99.6	99.1	99.5
0.101	0.7	0.9	1.4	99.3	99.1	98.6

According to Table 6, it is revealed that CO is produced mainly irrespective of p_{sweep} changing reaction temperature. Since reaction temperature is relatively lower even the reaction temperature of 600 °C and H_2 selectivity increases with an increase in reaction temperature, especially over 600 °C [32], high CO selectivity is obtained in this study.

Tables 7 and 8 list the relationship between CH_4, CO_2 conversion, H_2 yield and p_{sweep} changing moral ratio of CH_4:CO_2.

Table 7. Relationship between CH_4 conversion, CO_2 conversion and p_{sweep} changing molar ratios of CH_4:CO_2.

P_{sweep} (MPa)	CH_4 Conversion (%)			CO_2 Conversion (%)		
	CH_4:CO_2 = 1.5:1	CH_4:CO_2 = 1:1	CH_4:CO_2 = 1:1.5	CH_4:CO_2 = 1.5:1	CH_4:CO_2 = 1:1	CH_4:CO_2 = 1:1.5
0.045	0.129	0.231	0.047	35.2	33.5	22.2
0.090	0.112	0.162	0.072	40.1	27.8	20.6
0.101	0.193	0.178	0.105	39.4	29.0	9.85

Table 8. Relationship between H_2 yield and p_{sweep} changing molar ratios of CH_4:CO_2.

P_{sweep} (MPa)	H_2 Yield (%)		
	CH_4:CO_2 = 1.5:1	CH_4:CO_2 = 1:1	CH_4:CO_2 = 1:1.5
0.045	0.0322	0.0578	0.0117
0.090	0.0281	0.0405	0.0180
0.101	0.0483	0.0444	0.0262

According to Tables 7 and 8, it is seen that the CH_4 conversion and H_2 yield is the highest in the case of CH_4:CO_2 = 1:1, respectively. It is because the concentration of H_2 is the highest in the case of CH_4:CO_2 = 1:1, as shown in Figure 7. In addition, it is found from Table 7 that CO_2 conversion is higher than CH_4 conversion irrespective of molar ratio of CH_4:CO_2. Since the reactions shown by Equations (2) and (4) might be progressed well, this tendency is obtained.

3.3. Effect of Pressure of Sweep Gas on H_2 Flux from Reaction Chamber to Sweep Chamber

Figure 9 compares the impact of concentrations of H_2 at the outlet of the sweep chamber with changing reaction temperature. The reaction temperature is varied to 400 °C, 500 °C, or 600 °C. The error bars are also shown in this figure. It is seen from Figure 9 that the concentration of H_2 increases with a decrease in p_{sweep} irrespective of reaction temperature as expected. This is due to an increase in H_2 flux depending on the pressure difference between the reaction chamber and sweep chamber. In addition, the concentration of H_2 is the highest at the reaction temperature of 500 °C and p_{sweep} of 0.045 MPa. The reason is discussed as follows:

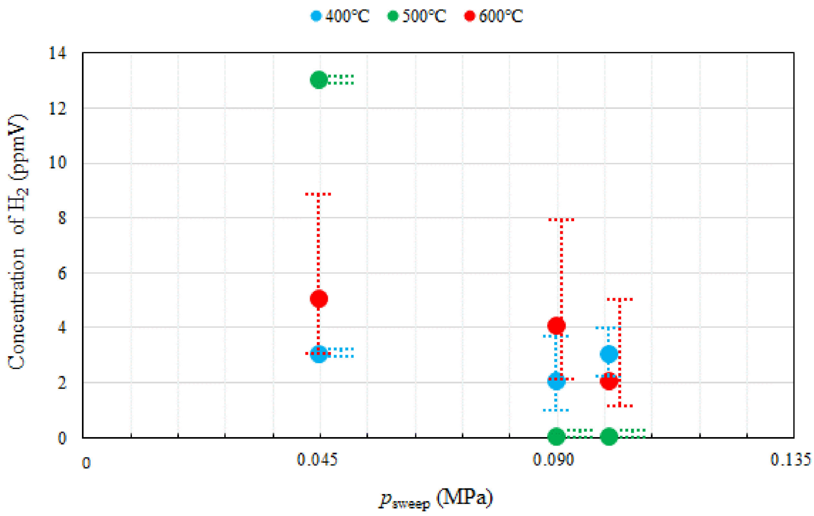

Figure 9. Impact of concentration of H_2 at the outlet of sweep chamber with p_{sweep} and reaction temperature.

In this study, the pressures of reaction chamber and sweep chamber have been measured by pressure sensors. The permeation flux through Pd/Cu membrane is calculated using the measured pressures of reaction chamber and sweep chamber as follows [52]:

$$J = \frac{Pe\left(\sqrt{p_{react}} - \sqrt{p_{sweep}}\right)}{\delta} \quad (13)$$

where J is the permeation flux (mol/(m^2·s)), Pe is the permeability and it is an inherent property of membrane (mol/(m·s·Pa$^{0.5}$)), p_{react} is the pressure of reaction chamber (MPa), p_{sweep} is the pressure of sweep chamber (MPa) and δ is the thickness of membrane (m). Pe of Pd/Cu membrane, used in this study, is listed in Table 9.

Table 9. *Pe* of Pd/Cu membrane used in this study [53].

Temperature (°C)	*Pe* (mol/(m·s·Pa$^{0.5}$))
400	1.0×10^{-8}
500	5.0×10^{-9}
600	1.0×10^{-9}

Figure 10 shows the impact of J and p_{sweep} with changing reaction temperature and molar ratio of CH_4:CO_2.

It is observed from Figure 10 that J increases with decrease in p_{sweep} irrespective of reaction temperature and molar ratio of CH_4:CO_2. It is due to an increase in the pressure difference between the reaction chamber and the sweep chamber. Additionally, it is found that J decreases with an increase in reaction temperature irrespective of p_{sweep} and molar ratio of CH_4:CO_2. According to Table 9, Pe of Pd/Cu membrane decreases with an increase in temperature, resulting that J decreases with an increase in reaction temperature.

In this study, J is the highest at the reaction temperature of 400 °C, while the amount of produced H_2 is the smallest at the reaction temperature of 400 °C due to a low kinetic production rate depending on temperature [54]. On the other hand, the amount of produced H_2 is the highest at the reaction temperature of 600 °C, while J is the lowest at the reaction temperature of 600 °C. Considering these tendencies, it can be thought that the reaction temperature of 500 °C is the optimum temperature, as shown in Figure 9.

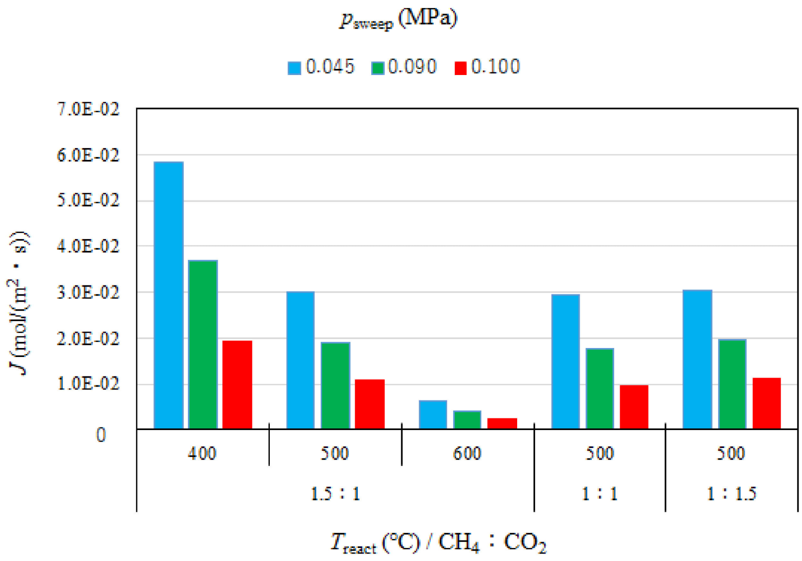

Figure 10. Impact of permeation flux with p_{sweep}, reaction temperature and molar ratios of CH_4:CO_2.

In this study, the performance of CH_4 dry reforming has not been high. According to the previous review paper on CH_4 dry reforming [55], CH_4 and CO_2 conversion were over 80%, though the reaction temperature was over 700 °C using several alloy catalysts, such as Ni/MgO, Ni/$Ce_{0.8}Zr_{0.2}O_2$, Ni/Co and Ni/CeO_2. The previous study also reported that not only CH_4 conversion, but also H_2 yield increased with an increase in the reaction temperature from 550 °C to 750 °C [56]. In addition, it was also reported that H_2 and CO yield increased with an increase in the reaction temperature from 450 °C to 700 °C, especially over 600 °C [32]. H_2 and CO yield attained at 30% and 45%, respectively at 700 °C [32]. Though the previous studies exhibited the better performance compared to this study, the reaction temperature is higher than this study. Reaction temperature is thought to be one essential parameter to decide the performance of CH_4 dry reforming, resulting that this study will investigate the higher reaction temperature condition in the near future. According to the numerical kinematic study on CH_4 steam reforming [57], which is one of the conventional approaches for H_2 production, the CH_4 conversion was approximately 65% at the reaction temperature of 650 °C and the pressure of 3.5 MPa with Ni/Al_2O_3 catalyst in a fixed bed reactor. In addition, the other experimental and numerical previous study on CH_4 steam reforming over NiO/Al_2O_3 catalyst [58] reported that the rate of CO formation increased with an increase in reaction temperature and almost all the CH_4 was converted to CO and H_2 at the reaction temperature of 800 °C. At 800 °C, CH_4 conversion, H_2 production rate and CO selectivity were 92.28%, 3.34% and 99%, respectively. It can be also known from these references on the conventional approach for H_2 production that reaction temperature is an important parameter to improve the performance of H_2 production.

It is necessary to improve the performance of CH_4 dry reforming from the view point of reaction kinetics and H_2 separation. Though only pure Ni catalyst has been investigated in this study, Ni-based alloy catalysts, such as Ni/Ce [6], Ni/La [6] and Ni/ZnO-Al_2O_3 [17] exhibited the better performance, and they are promising candidate catalysts for further studies. In addition, the characterization of H_2 separation membrane, such as composition, thickness, and metal type, is important to improve the efficiency of H_2 separation. Since this study has investigated one type of H_2 separation membrane only, i.e., Pd/Cu alloy membrane (Cu of 40 wt%) whose thickness is 60 µm, the different composition and thinner membrane will also be investigated in the near future.

In addition, the control of pressure difference between reaction chamber and sweep chamber is important to improve the performance of H_2 separation membrane. The numerical analysis on biogas dry reforming membrane reactor reported that the system efficiency, which was defined by the ratio of H_2 energy output to biogas and auxiliaries energy inputs, increased with an increase in the pressure difference between reaction chamber and sweep chamber, and H_2 production efficiency was attained around 69 % at the pressure difference of 20 bar (=0.2 MPa) [59]. Since the pressure difference provided by this study is up to 0.055 MPa, it might be desirable to investigate the higher pressure difference in order to improve the proposed membrane reactor.

Finally, this study suggests optimizing the catalyst, H_2 separation membrane and operation condition in order to obtain a progress compared to other similar studies.

4. Conclusions

This study has studied the effect of p_{sweep} on the performance of biogas dry reforming. This study has investigated the effect changing the reaction temperature from 400 °C to 600 °C, and the molar ratio of CH_4:CO_2 by 1.5:1, 1:1 and 1:1.5, where the molar ratio of CH_4:CO_2 = 1.5:1 simulates a biogas. As a result, the following conclusions are drawn from the obtained results:

(i) Under the condition of the molar ratio of CH_4:CO_2 = 1.5:1 changing the reaction temperature by 400 °C, 500 °C, 600 °C, the impact of p_{sweep} on concentrations of CH_4 and CO at the outlet of reaction chamber is negligible. It is concluded that the concentrations of H_2 and CO at the outlet of reaction chamber increase with incase in the reaction temperature. It is revealed that the concentration of H_2 at the outlet of reaction chamber, under negative pressure conditions, is smaller than that under the atmosphere pressure condition. High CO selectivity is obtained, while H_2 selectivity is low.

(ii) Under the condition of the reaction temperature of 500 °C changing molar ratio of CH_4:CO_2, the highest concentration of H_2 at the outlet of reaction chamber is obtained at the molar ratio of CH_4:CO_2 = 1:1. In addition, the concentrations of H_2 at the outlet of reaction chamber under negative pressure conditions are lower than those under the atmosphere pressure condition, except for the case of the molar ratio of CH_4:CO_2 = 1:1. The concentration of CO at the outlet of reaction chamber is the highest in the case of the molar ratio of CH_4:CO_2 = 1.5:1. High CO selectivity is obtained, while H_2 selectivity is low.

(iii) CO_2 conversion is larger compared to CH_4 conversion irrespective of p_{sweep}, reaction temperature and molar ratio of CH_4:CO_2. CH_4 conversion and H_2 yield is the highest in the case of CH_4:CO_2 = 1:1, respectively.

(iv) The concentration of H_2 at the outlet of sweep chamber is the highest at the reaction temperature of 500 °C and p_{sweep} of 0.045 MPa. It is due to the balance between the permeation flux and reaction kinetics.

According to the investigation by this study, it is necessary to improve the performance of CH_4 dry reforming from the view point of reaction kinetics and H_2 separation. Ni-based alloy catalyst is a promising catalyst in order to improve the performance of CH_4 dry reforming. In addition, it is important to clarify the impact of the characterization of H_2 separation membrane, such as composition, thickness, and metal type, on the efficiency of H_2 separation. Furthermore, it is also important to control the pressure difference between reaction chamber and sweep chamber in order to improve the performance of the H_2 separation membrane.

Author Contributions: Conceptualization, A.N.; experiment and data curation, T.T. and S.O.; writing—original draft preparation, A.N.; writing—review and editing, M.L.K. All authors have read and agreed to the published version of the manuscript.

Funding: This research was funded by the joint research program of the Institute of Materials and Systems for Sustainability, Nagoya University and the Tatematsu Foundation, Japan.

Institutional Review Board Statement: Not applicable.

Informed Consent Statement: Not applicable.

Data Availability Statement: The data presented in this study are openly available.

Conflicts of Interest: The authors declare no conflict of interest.

References

1. Tinnirello, M.; Papurello, D.; Santarelli, M.; Fiorilli, S. Thermal activation of digested sewage sludges for carbon dioxide removal from biogas. *Fuels* **2020**, *1*, 30–46. [CrossRef]
2. Kuan, C.Y.; Neng, M.L.Y.; Chan, Y.B.; Sim, Y.L.; Strothers, J.; Pratt, L.M. Thermal transformation of plan waste to high-quality hydrocarbon fuel. *Fuels* **2020**, *1*, 2–14. [CrossRef]
3. Karatza, D.; Konstantopoulos, C.; Chianese, S.; Diplas, S.; Svec, P.; Hristoforou, E.; Musmarra, D. Hydrogen production through water splitting at low temperature over Fe_3O_4 pellet: Effects of electric power, magnetic field, and temperature. *Fuel Process. Technol.* **2021**, *211*, 106606. [CrossRef]
4. Guo, S.; Li, X.; Li, J.; Wei, B. Boosting photocatalytic hydrogen production from water by photothermally induced biphase systems. *Nat. Commun.* **2021**, *12*, 1–10. [CrossRef]
5. Vinvent, I.; Lee, E.C.; Kim, H.M. Comprehensive impedance investigation of low-cost anion exchange membrane electrolysis for large-scale hydrogen production. *Sci. Rep.* **2021**, *11*, 1–12. [CrossRef]
6. Kalai, D.Y.; Stangeland, K.; Jin, Y.; Tucho, W.M.; Yu, Z. Biogas dry reforming for syngas production on La promoted hydrotalcite-derived Ni catalyst. *Int. J. Hydrog. Energy* **2018**, *43*, 19438–19450. [CrossRef]
7. World Bioenergy Association. Global Bioenergy Statistics. Available online: https://worldbioenergy.org./global-bioenergy-statistics (accessed on 23 March 2021).
8. The Japan Gas Association. Available online: https://www.gas.or.jp/gas-life/biomass/ (accessed on 23 March 2021).
9. Foo, S.Y.; Cheng, C.K.; Nguyen, T.H.; Adesina, A.A. Kinetic study of methane CO_2 reforming on Co-Ni/Al_2O_3 and Ce-Co-Ni/Al_2O_3 catalysts. *Catal. Today* **2011**, *164*, 221–226. [CrossRef]
10. Bobrova, L.N.; Bobin, A.S.; Mezentseva, N.V.; Sadykov, V.A.; Thybaut, J.W.; Marin, G.B. Kinetic assessment of dry reforming of methane on Pt + Ni containing composite of fluorite-like structure. *Appl. Catal. B Environ.* **2016**, *182*, 513–524. [CrossRef]
11. Park, N.; Park, M.J.; Baek, S.C.; Ha, K.S.; Lee, Y.J.; Kwak, G.; Park, H.G.; Jun, K.W. Modeling and optimization of the mixed reforming of methane: Maximizing CO_2 utilization for non-equilibrated reaction. *Fuel* **2014**, *115*, 357–365. [CrossRef]
12. Ozkara-Aydinoglu, S.; Aksoylu, A.E. A comparative study on the kinetics of carbon dioxide reforming of methane over Pt-Ni/Al_2O_3 catalyst: Effect of Pt/Ni ratio. *Chem. Eng. J.* **2013**, *215–216*, 542–549. [CrossRef]
13. Li, K.; He, F.; Yu, H.; Wang, Y.; Wu, Z. Theoretical study on the reaction mechanism of carbon dioxide reforming of methane on La and La_2O_3 modified Ni (1 1 1) surface. *J. Catal.* **2018**, *364*, 248–261. [CrossRef]
14. Elsayed, N.H.; Roberts, N.R.M.; Joseph, B.; Kuhn, J.N. Comparison of Pd-Ni-Mg/Ceria-Zirconia and Pt-Ni-Mg/Ceria-Zirconia catalysts for syngas production via low temperature forming of model biogas. *Top. Catal.* **2016**, *59*, 138–146. [CrossRef]
15. Shang, Z.; Li, S.; Li, L.; Liu, G.; Liang, X. Highly active and stable alumina supported nickel nanoparticle catalysts for dry reforming of methane. *Appl. Catal. B Environ.* **2017**, *201*, 302–309. [CrossRef]
16. Omoregbe, O.; Danh, H.T.; Nguyen-Huy, C.; Setiabudi, H.D.; Abidin, S.Z.; Truong, Q.D.; Vo, D.V.N. Syngas production from methane dry reforming over Ni/SBA-15 catalyst: Effect of operating parameters. *Int. J. Hydrog. Energy* **2017**, *42*, 11283–11294. [CrossRef]
17. Nataj, S.M.M.; Alavi, S.M.; Mazloom, G. Catalytic performance of Ni supported on ZnO-Al_2O_3 composites with different Zn content in methane dry reforming. *J. Chem. Technol. Biotechnol.* **2019**, *94*, 1305–1314. [CrossRef]
18. Yan, X.; Hu, T.; Liu, P.; Li, S.; Zhao, B.; Zhang, Q.; Jiao, W.; Chen, S.; Wang, P.; Lu, J.; et al. Highly efficient and stable Ni/CeO_2-SiO_2 catalyst for dry reforming of methane: Effect of interfacial structure of Ni/CeO_2 on SiO_2. *Appl. Catal. B Environ.* **2019**, *246*, 221–231. [CrossRef]
19. Zhang, M.; Zhang, J.; Wu, Y.; Pan, J.; Zhang, Q.; Tan, Y.; Han, Y. Insight into the effects of the oxygen species over Ni/ZrO_2 catalyst surface on methane reforming with carbon dioxide. *Appl. Catal. B Environ.* **2019**, *244*, 427–437. [CrossRef]
20. Park, J.H.; Heo, I.; Chang, T.S. Dry reforming of methane over Ni-substituted CaZrNiOx catalyst prepared by the homogeneous deposition method. *Catal. Commun.* **2019**, *120*, 1–5. [CrossRef]
21. Hossain, M.A.; Ayodele, B.V.; Cheng, C.K.; Khan, M.R. Optimization of renewable hydrogen-rich syngas production from catalytic reforming of greenhouse gases (CH_4 and CO_2) over calcium iron oxide supported nickel catalyst. *J. Energy Inst.* **2019**, *92*, 177–194. [CrossRef]
22. Rosha, P.; Mohapatra, S.K.; Mahla, S.K.; Dhir, A. Biogas reforming for hydrogen enrichment by ceria decorated over nickel catalyst supported on titania and alumina. *Int. J. Hydrog. Energy* **2018**, *43*, 21246–21255. [CrossRef]
23. Rosha, P.; Mohapatra, S.K.; Mahla, S.K.; Dhir, A. Hydrogen enrichment of biogas via dry and authothermal-dry reforming with pure nickel (Ni) nanoparticle. *Energy* **2019**, *172*, 733–739. [CrossRef]
24. Rosha, P.; Mohapatra, S.K.; Mahla, S.K.; Dhir, A. Catalytic reforming of synthetic biogas for hydrogen enrichment over Ni supported on ZnO-CeO_2 mixed catalyst. *Biomass Bioenergy* **2019**, *125*, 70–78. [CrossRef]
25. Schiaroli, N.; Lucarelli, C.; Luna, G.S.; Fornasari, G.; Vaccari, A. Ni-based catalysts to produce synthesis gas by combined reforming of clean biogas. *Appl. Catal. A Gen.* **2019**, *582*, 117087. [CrossRef]
26. Lyu, L.; Han, Y.; Ma, Q.; Makpal, S.; Sun, J.; Gao, X.; Zhang, J.; Fan, H.; Zhao, T.S. Fabrication of Ni-based bimodal porous catalyst for dry reforming of methane. *Catalysts* **2020**, *10*, 1220. [CrossRef]

27. Omran, A.; Yoon, S.H.; Khan, M.; Ghouri, M.; Chatla, A.; Elbashir, N. Mechanistic insights for dry reforming of methane on Cu/Ni bimetallic catalysts: DFT-assisted microkinetic analysis for coke resistance. *Catalysts* **2020**, *10*, 1043. [CrossRef]
28. Anzelmo, B.; Wilcox, J.; Liguori, S. Natural gas stream reforming reaction at low temperature and pressure conditions for hydrogen production via Pd/PSS methane reactor. *J. Membr. Sci.* **2017**, *522*, 343–350. [CrossRef]
29. Yan, Y.; Cui, Y.; Zhang, J.; Chen, Y.; Tang, Q.; Lin, C. Experimental investigation of methane auto-thermal reforming in hydrogen-permeable membrane reactor for pure hydrogen production. *Int. J. Hydrog. Energy* **2016**, *41*, 13069–13076. [CrossRef]
30. Dolan, M.; Beath, A.; Hla, S.; Way, J.; Abu El Hawa, H. An experimental and techno-economic assessment of solar reforming for H_2 production. *Int. J. Hydrog. Energy* **2016**, *41*, 14583–14595. [CrossRef]
31. Brunetti, A.; Fontananova, E. CO_2 conversion by membrane reactors. *J. Nanosci. Nanotechnol.* **2019**, *19*, 3124–3134. [CrossRef]
32. Sumrunronnasak, S.; Tantayanon, S.; Kiatgamolchai, S.; Sukonket, T. Improved hydrogen production from dry reforming reaction using a catalytic packed-bed membrane reactor with Ni-based catalyst and dense PdAgCu alloy membrane. *Int. J. Hydrog. Energy* **2016**, *41*, 2621–2630. [CrossRef]
33. Duran, P.; Sanz-Martinez, A.; Soler, J.; Manendez, M.; Herguido, J. Pure hydrogen from biogas: Intensified methane dry reforming in a two-zone fluidized bed reactor using permselective membranes. *Chem. Eng. J.* **2019**, *370*, 772–781. [CrossRef]
34. Bosko, M.L.; Munera, J.F.; Lombardo, E.A.; Cornaglia, L.M. Dry reforming of methane in membrane reactors using Pd and Pd-Ag composite membranes on a NaA zeolite modified porous stainless steel support. *J. Membr. Sci.* **2010**, *364*, 17–26. [CrossRef]
35. Munera, J.; Faroldi, B.; Fruits, E.; Lombardo, E.; Cornaglia, L.; Carrazan, S.G. Supported Rh nanoparticles on CaO-SiO_2 binary systems for the reforming of methane by carbon dioxide in membrane reactors. *Appl. Catal. A Gen.* **2014**, *474*, 114–124. [CrossRef]
36. Simakov, D.S.A.; Roman-Leshkov, Y. Highly efficient methane reforming over a low-loading Ru/-Al_2O_3 catalyst in a Pd-Ag membrane reactor. *AICHE J.* **2018**, *64*, 3101–3108. [CrossRef]
37. Liu, J.; Bellini, S.; Nooijer, N.C.A.; Sun, Y.; Tanaka, D.A.P.; Tang, C.; Li, H.; Gallucci, F.; Caravella, A. Hydrogen permeation and stability in ultra-thin Pd-Ru supported membrane. *Int. J. Hydrog. Energy* **2020**, *45*, 7455–7467. [CrossRef]
38. Fontana, A.D.; Faroldi, B.; Cornaglia, L.M.; Tarditi, A.M. Development of catalytic membranes over PdAu selective films for hydrogen production through the dry reforming of methane. *Mol. Catal.* **2020**, *481*, 100643. [CrossRef]
39. Jia, H.; Xu, H.; Sheng, X.; Yang, X.; Shen, W.; Goldbach, A. High-temperature ethanol steam reforming in PdCu membrane reactor. *J. Membr. Sci.* **2020**, *605*, 118083. [CrossRef]
40. Roa, F.; Way, D. Influence of alloy composition and membrane fabrication on the pressure dependence of the hydrogen flux of palladium-copper membranes. *Ind. Eng. Chem. Res.* **2003**, *42*, 5827–5835. [CrossRef]
41. Garcia-Garcia, F.R.; Soria, M.A.; Mateos-Pedero, C.; Guerrero-Ruiz, A.; Odriguez-Ramos, I.; Li, K. Dry reforming of methane using Pd-based membrane reactors fabricated from different substrates. *J. Membr. Sci.* **2013**, *435*, 218–225. [CrossRef]
42. Ugarte, P.; Duran, P.; Lasobras, J.; Soler, J.; Menendez, M.; Herguido, J. Dry reforming of biogas in fluidized bed; process intensification. *Int. J. Hydrog. Energy* **2017**, *42*, 13589–13597. [CrossRef]
43. Kumar, S.; Kumar, B.; Kumar, S.; Jilani, S. Comparative modeling study of catalytic membrane reactor configurations for syngas production by CO_2 reforming of methane. *J. CO_2 Util.* **2017**, *20*, 336–346. [CrossRef]
44. Leimert, J.M.; Karl, J.; Dillig, M. Dry reforming of methane using a nickel membrane reactor. *Processes* **2017**, *5*, 82. [CrossRef]
45. Ben-Mansour, R.; Abuelyamen, A.; Habib, M.A. CFD modeling of hydrogen separation through Pd-based membrane. *Int. J. Hydrog. Energy* **2020**, *45*, 23006–23019. [CrossRef]
46. Li, H.; Goldbach, A.; Li, W.; Xu, H. PdC formation in ultra-thin Pd membrane during separation of H_2/CO mixtures. *Int. J. Hydrog. Energy* **2016**, *41*, 10193–10201. [CrossRef]
47. Nishimura, A.; Ohata, S.; Okukura, K.; Hu, E. The Impact of Operating Conditions on the Performance of a CH4 Dry Reforming Membrane Reactor for H2 Production. *J. Energy Power Technol.* **2020**, *2*, 1–19. [CrossRef]
48. Zhang, J.; Wang, H.; Dalai, A.K. Kinetic studies of carbon dioxide reforming of methane over Ni-Co/Al-Mg-O bimetallic catalyst. *Ind. Eng. Chem. Res.* **2009**, *48*, 677–684. [CrossRef]
49. Avetisov, A.K.; Rostrup-Nielsen, J.R.; Kuchaev, V.L.; Hansen, J.H.B.; Zyskin, A.G.; Shapatina, E.N. Steady-state kinetics and mechanism of methane reforming with steam and carbon dioxide over Ni catalyst. *J. Mol. Catal. A Chem.* **2010**, *315*, 155–162. [CrossRef]
50. Richardson, J.T.; Paripatyadar, S.A. Carbon dioxide reforming of methane with supported rhodium. *Appl. Catal.* **1990**, *61*, 293–309. [CrossRef]
51. Quiroga, M.M.B.; Luna, A.E.C. Kinetic analysis of rate data for dry reforming of methane. *Ind. Eng. Chem. Res.* **2007**, *46*, 5265–5270. [CrossRef]
52. Benguerba, Y.; Virginie, M.; Dumas, C.; Ernst, B. Computational fluid dynamics study of the dry reforming of methane over Ni/Al_2O_3 catalyst in membrane reactor. Coke deposition. *Kinet. Catal.* **2017**, *58*, 328–338. [CrossRef]
53. Tsuneki, T.; Shirasaki, Y.; Yasuda, I. Hydrogen permeability of palladium-copper alloy membranes. *J. Jpn. Inst. Met.* **2006**, *70*, 658–661. [CrossRef]
54. Fan, M.S.; Abdullah, A.Z.; Bhatia, S. Utilization of greenhouse gases through dry reforming: Screening of nickel-based bimetallic catalysts and kinetic studies. *ChemSusChem* **2011**, *4*, 1643–1653. [CrossRef]
55. Jang, W.J.; Shim, J.O.; Kim, H.M.; Yoo, S.Y.; Roh, H.S. A review on dry reforming of methane in aspect of catalytic properties. *Catal. Today* **2019**, *324*, 15–26. [CrossRef]

56. Lee, B.; Lim, H. Parametric studies for CO_2 reforming of methane in a membrane reactor as a new CO_2 utilization process. *Korean J. Chem. Eng.* **2017**, *34*, 199–205. [CrossRef]
57. Neni, A.; Benguerba, Y.; Balsamo, M.; Erto, A.; Ernst, B.; Benachour, D. Numerical study of sorption-enhanced methane steam reforming over Ni/Al_2O_3 catalyst in a fixed-bed reactor. *Int. J. Heat Mass Transf.* **2021**, *165*, 120635. [CrossRef]
58. Chen, K.; Zhao, Y.; Zhang, W.; Feng, D.; Sun, S. The intrinsic kinetics of methane steam reforming over a nickel-based catalyst in a micro fluidized bed reaction system. *Int. J. Hydrog. Energy* **2020**, *45*, 1615–1628. [CrossRef]
59. Marcoberardino, G.D.; Foresti, S.; Binotti, M.; Manzolini, G. Potentiality of a biogas membrane reformer for decentrailized hydrogen production. *Chem. Eng. Process. Process Intensif.* **2018**, *129*, 131–141. [CrossRef]